

Ab initio calculation of the electronic structure of thallos halides. II. One-particle states: Wannier functions, band structures, and densities of states

M. Schreiber and W. Schäfer

Institut für Physik, Universität Dortmund, D-4600 Dortmund 50, West Germany

(Received 9 May 1983)

Ground-state charge densities, which have been calculated *ab initio* self-consistently and determined by minimization of the total energy, are used for a self-consistent calculation of the one-particle states of simple-cubic thallos chloride and thallos bromide, taking into account the self-energy corrections computed in the local-density-functional approximation. We depict the resulting wave functions in a Wannier basis; the band structure is analyzed, and direct and indirect gaps are shown to be in good agreement with experiments and allow a quantitative explanation of the unusual pressure coefficients and deformation potentials of the thallos halides. The derived valence-band densities of states are confirmed in all details by various photoemission experiments; the conduction-band density of states of thallos chloride is corroborated by experiments on core-level spectroscopy. The unusual polarization properties of thallos halides are attributed to the existence of the inert *s*-electron pair (of the cation) beyond the closed-shell configuration of the compound. The relevance of self-energy and self-interaction corrections is discussed.

I. INTRODUCTION

Compound semiconductors of the types $A^{III}B^{VII}$, $A^{IV}B^{VI}$, $A^{IV}B_2^{VII}$, $C^IA^{IV}B_3^{VII}$, etc., such as $TlCl$, $PbTe$, PbI_2 , and $CsPbCl_3$, are distinguished from the "usual" A^NB^{8-N} semiconductors such as $GaAs$, $ZnSe$, and Ge , because the outermost *s* orbital of the cation *A* is occupied beyond the closed-shell configuration. In the so-called "ten-electron" compounds, as well as in the more complex structures mentioned above, this "inert *s*-electron pair" of the cation forms the valence band together with anionic *p* states, while the energetically lowest conduction bands are dominated by cationic *p* states. As a result, the electronic properties show characteristic differences from other ionic or covalent compounds¹ as follows: A rather small band gap situated at the edge of the Brillouin zone with a predominantly intracationic exciton, as a consequence of the small gap a high polarizability which is characterized in the optical region by charge-transfer transition from *B* to *A* as well as intracationic transitions; the easily deformable, i.e., polarizable outermost *s* subshell leads to unusually large and negative pressure coefficients of the lowest optical transitions; it also causes the unusually large static screening and strong electron-phonon coupling.

It is the purpose of this paper to describe an *ab initio* calculation of the one-electron states of the simplest compounds with an inert *s*-electron pair, namely the thallos halides. This investigation is based on the previously reported self-consistent *ab initio* calculation of the electronic ground state of thallos halides² (hereafter referred to as I), which employed the local-density-functional (LDF) formalism.^{3,4}

However, it is well known^{5,6} that the Schrödinger equation which follows from the LDF-ground-state formalism by a variational principle with respect to the density is solved by eigenvalues which do not obey Koopmans's theorem⁷; therefore an interpretation of these eigenvalues

and the corresponding eigenfunctions as one-particle states is strictly speaking unjustified, although not uncommon.⁸⁻¹⁰ The necessary investigation of the Dyson equation for the one-particle Green's function leads in a local approximation of the self-energy to an appropriate one-particle equation which differs from the ground-state Schrödinger equation only by a local energy-dependent potential.⁵ These so-called self-energy corrections have been self-consistently taken into account in the usual local approximation.⁶ The analysis of the resulting band structures and densities of states shows good agreement with optical as well as photoemission spectra.

Although the basic variable of the LDF formalism is the charge density, it is often advantageous or even necessary, e.g., for the investigation of many-body corrections to optical spectra,¹¹ to gain detailed knowledge of the wave functions. Usually, a particularly useful basis is provided by the Wannier functions¹² because of their strong localization and orthogonality. Until now, however, this convenient and physically intuitive basis has been used nearly exclusively for theoretical considerations or simple model calculations.¹³ We employ a construction scheme which allows a simple construction even for crossing bands. We have adapted this scheme, which was developed in the framework of Hartree-Fock calculations,¹⁴ to the LDF formalism and used it in a previous investigation of thallos chloride.¹⁵ After a recapitulation of the basic equations we present the final Wannier functions in the next section and compare it with other representations of the one-particle wave functions. We then explain the self-consistent determination of the one-particle energies for simple cubic thallos chloride and bromide; the resulting band structures are discussed in the Sec. III. They are more accurate than the $TlCl$ band structure presented in the previous investigation¹⁵ because the calculation of the underlying ground state has been improved considerably. They now allow an analysis of the lowest

optical transitions including the pressure coefficients. In the final section the densities of states are compared with various photoemission spectra. The discussion of these data shows that many of the unusual characteristics of thallos halides can be explained by the existence of the inert *s*-electron pair.

II. CALCULATION OF THE ONE-PARTICLE STATES

A. Schrödinger equation

In principle, the calculation of excited states of an *N*-particle system requires the solution of the Dyson equation.⁵ The resulting one-particle Green's function yields one-particle energies which represent the energy difference between the *N*- and the (*N* ± 1)-electron systems and thus allow the determination of the band-structure and excitation energies. Within the LDF formalism, which we employ in the present investigation, the self-energy in the Dyson equation is locally approximated by the self-energy of an homogeneous electron gas,⁵ which is known from dynamically screened Hartree-Fock calculations.¹⁶ This approximation leads to the following Schrödinger equation:

$$[-\Delta + V_C(r) + V_{xc}(\rho(r), E) - E_m(E)]\Psi_m(r, E) = 0, \quad (1)$$

where the effective exchange-correlation potential V_{xc} describes the energy-dependent self-energy.

At $E = \mu_N$, the chemical potential of the *N*-particle system, it coincides with the exchange-correlation potential μ_{xc} of the ground-state formalism which was discussed in I. We therefore set

$$V_{xc}(\rho, E) = \mu_{xc}(\rho) + \Delta\Sigma(\rho, E). \quad (2)$$

Thus the Schrödinger equation for the excited states differs from the ground-state equation only by the additional energy-dependent potential $\Delta\Sigma$, the so-called self-energy corrections. Employing the charge density which resulted from the determination of the ground state in I, we can easily determine¹⁷ the self-energy corrections and then solve the Schrödinger equation (1) to derive the one-particle energies E_m and wave functions Ψ_m .

B. Representation of the wave functions

A conceptually simple and intuitive basis for the representation of the one-particle wave functions was originally defined by Wannier.¹² The Wannier functions are normalized and orthogonal, localized within the unit cell and decay exponentially if they describe an isolated band. However, the computations as Fourier transforms of the Bloch functions of a single band requires first the solution of the adequate Schrödinger equation. For connected bands this specification leads to Wannier functions which decay only with an inverse power,¹⁸ because the Bloch functions are no longer analytic at the crossing points of the bands. As an example, Fig. 1 shows the Wannier function which was calculated for the upper valence band of thallos chloride from the Bloch functions which solve the Schrödinger equation (1). A very complicated function results with a rather slow decay proportional to $1/r$ [note that $ra(r)$ is plotted].

A simple construction scheme which avoids these problems was given by Kohn¹⁴ but rarely used.^{8,19} Exponentially decaying Wannier functions even for connected bands without prior knowledge of the Bloch functions are obtained from a set of localized functions ψ_i ,

$$a_{iL}(r) = N^{-1/2} \sum_l \sum_j \sum_k e^{ikl} \psi_j(r-l-L) b_{ji}(k). \quad (3)$$

To derive orthogonal normalized Wannier functions the coefficients have to satisfy

$$b_{ji}(k) = S_{ji}^{-1/2}(k), \quad (4)$$

where S_{ji} denotes the overlap matrix between the Bloch-symmetrized basis functions,

$$S_{ji}(k) = \sum_L \left[\int \psi_i(r) \psi_j(r-L) dr \right] e^{ikL} = \sum_L S_{jiL} e^{ikL}. \quad (5)$$

This orthogonalization scheme, which was already given by Löwdin,²⁰ does not change the symmetry properties. Therefore the Wannier functions transform according to the point group of the crystal if we demand this symmetry for the basis ψ_i . However, the Wannier functions are not uniquely defined in this way because the square root of a matrix [in Eq. (4)] is not. If we start from a nearly orthogonal basis, i.e.,

$$D_{ij}(k) = S_{ij}(k) - \delta_{ij} \approx 0, \quad (6)$$

we can suitably use the fast-converging series

$$S^{-1/2}(k) = 1 - \frac{1}{2}D(k) + \frac{3}{8}D^2(k) - \frac{5}{16}D^3(k) + \dots \quad (7)$$

to obtain Wannier functions which differ from the localized basis only by a small correction

$$a_{jL}(r) = \psi_j(r-L) - \frac{1}{2} \sum_{i,L'} \psi_i(r-L') \times \int dr' \psi_j(r'-L) \psi_i(r'-L') + \dots \quad (8)$$

In Fig. 2 we present a Wannier function $a_{j0}(r)$ constructed

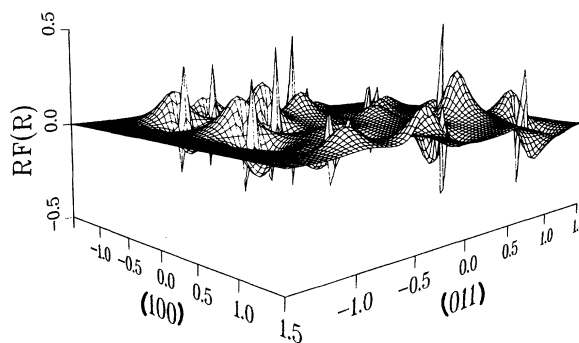


FIG. 1. Wannier function $F(R)$ of the upper valence band located at a chlorine ion calculated as Fourier transform of the Bloch functions of this band. Note the scale: In order to display the off-center contributions the function was scaled up by a factor R .

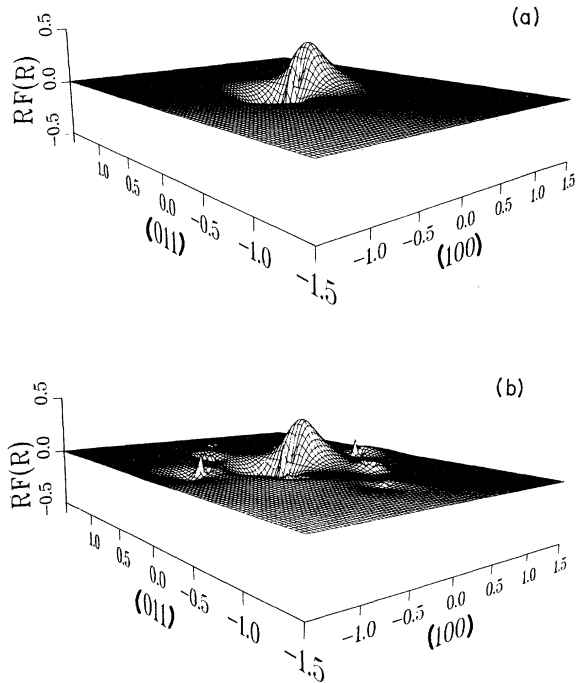


FIG. 2. (a) Basis function with p symmetry localized at a chlorine ion. (b) Corresponding Wannier function calculated according to the Löwdin scheme [Eq. (8)] by orthogonalization of the localized orbital (a) on all functions which contribute to valence and conduction bands. Scale is the same as in Fig. 1.

according to this scheme and its starting point, the localized orbital ψ_j . The difference is very small and only noticeable near the neighboring lattice sites where the orbitals ψ_{iL} are localized. Obviously this generalized Wannier function is much better localized than the straightforwardly calculated function in Fig. 1.

In general [i.e., relaxing the condition (6)], the generalized Wannier functions are obtained directly from a super-

position of the Bloch-symmetrized local orbitals ψ_j according to definition (3). Figure 3 shows a Bloch-symmetrized local orbital for various wave vectors. Only the contribution localized at the origin does not change, all other contributions oscillate, so that the summation in Eq. (3) over all wave vectors yields an exponentially localized Wannier function.

C. Basis set

In view of the similarity between the Schrödinger equation (1) and the quasiparticle equation of the LDF—ground-state formalism, we use the optimized basis set of localized orbitals which followed from the minimization of the total energy with respect to the basis set.²¹ That means we take the orbitals of the free ions up to $5d\text{-Tl}^+$, $3s\text{-Cl}^-$, and $4s\text{-Br}^-$ as frozen core and the $6s$ - and $6p\text{-Tl}^+$, $3p\text{-Cl}^-$, and $4p\text{-Br}^-$ orbitals with varied outermost maxima for the description of valence and conduction states. With respect to the total energy the thus-defined frozen core turned out to be a reasonable approximation causing only small errors.² With regard to the band structure, the implications of the frozen core should be insignificant as can be seen from the energetically uppermost orbitals which are included in the core, namely, $5d_{3/2}$ and $5d_{5/2}$ of thallium about 10 eV below the valence bands. Their energy levels do not display any crystal-field splitting which should arise if the ionic orbitals are influenced by their environment. While this effect was observed, e.g., in photoemission spectra of silver halides,²² the thallous halide spectra display only a spin-orbit splitting of 2.31 eV in TlCl and 2.27 eV in TlBr (Ref. 23) which agrees within experimental error with the splitting of the $5d$ energies of free Tl^+ ions known from experiment²³ and relativistic calculations.²⁴ These experiments confirm that the one-particle energies corresponding to these core functions are not significantly influenced by the formation of the crystal. However, in order to avoid any mixing terms between core and other states in the secular

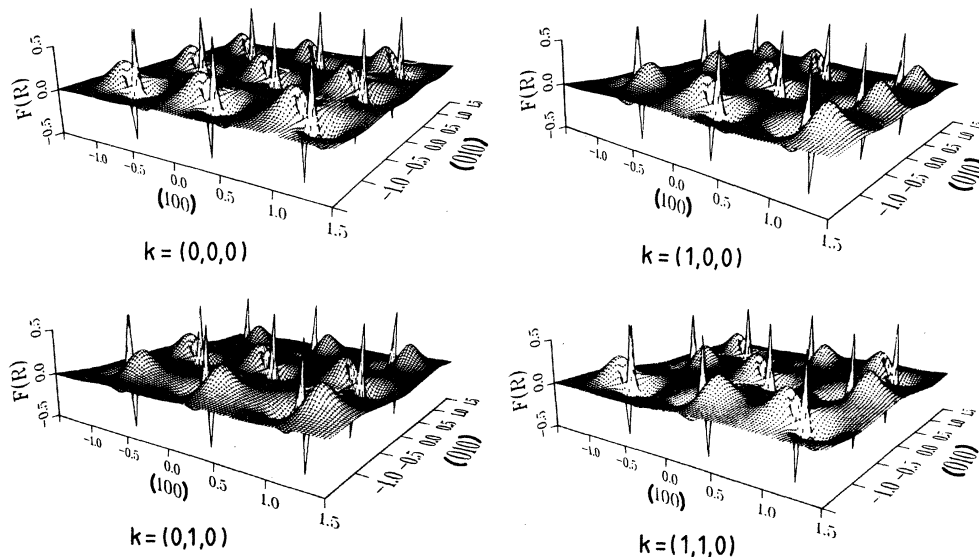


FIG. 3. Localized basis function of Fig. 2(a) after Bloch symmetrization for different wave vectors \vec{k} .

equation corresponding to the Schrödinger equation (1), we have explicitly orthogonalized the "other" states on all core states using the usual Schmidt procedure.

The overlap matrix $S_{ij}(k)$ [Eq. (5)] and the corresponding Hamiltonian matrix $H_{ij}(k)$ among valence and conduction orbitals are thus corrected,

$$S_{ij}^0(k) = S_{ij}(k) - \sum_c S_{ic}^*(k) S_{cj}(k),$$

$$H_{ij}^0(k) = H_{ij}(k) - \sum_c S_{ic}^*(k) E_c(k) S_{cj}(k),$$

where the sum runs over all core orbitals, and S_{ij} , S_{ic} , and S_{cj} are defined by Eq. (5). From the above argument that the formation of the crystal hardly changes the core, it follows that the core-energy levels E_c are nearly dispersionless and can therefore be approximated by the levels of the free ions appropriately shifted by the Madelung energy. We have calculated the neglected dispersion effects non-self-consistently and found that the contributions of various core states largely cancel, and significant changes of the order of 0.1 eV occur only at the extrema of the bands, yielding, e.g., an increase of the band gap by 0.25 eV. On the other hand, considering the uppermost conduction states which follow from the described basis set, we cannot expect to achieve a very good basis-set convergence. For these states we estimate that the mixing of higher orbitals changes the one-particle energies up to 0.5 eV.

D. Self-consistent solution of the Schrödinger equation

From the Schrödinger equation (1) we derive the secular equation in terms of the localized orbitals in the usual way,

$$\det \left[\sum_L [H_{ijL}^0(k) + \Delta \Sigma_{ijL}(E, k) - E S_{ijL}^0(k)] e^{ikL} \right] = 0, \quad (9)$$

where the matrix elements are calculated between the core-orthogonalized localized orbitals $\psi_i(r)$ and $\psi_j(r-L)$, and H^0 represents the Hamiltonian of the ground-state equation including relativistic corrections for the mass-velocity and Darwin terms and the spin-orbit coupling.²⁵ Owing to the energy dependence of the self-energy corrections this eigenvalue problem is nonlinear and has to be solved self-consistently with respect to the energy. Although this self-consistency does affect the wave functions, it should be noted that in the LDF formalism, the charge density, which enters the calculation of the matrix elements, has to be taken from the ground state and is therefore not affected. Hence we can determine the matrix elements of the self-energy corrections in Eq. (9) for all energies from the ground-state charge density. It turned out^{15,17} that the matrix elements of the self-energy corrections depend approximately linearly on the energy,

$$\Delta \Sigma_{ijL} = \sigma_{ijL}^{\pm} E, \quad (10)$$

with different proportionality constants σ^+ and σ^- for energies above and below the chemical potential. We can therefore reduce the problem to a secular equation which is linear in the energy,

$$\det \left[\sum_L e^{ikL} \{ H_{ijL}^0(k) - E [S_{ijL}^0(k) - \sigma_{ijL}^{\pm}(k)] \} \right] = 0. \quad (11)$$

This is nothing but the secular equation of the ground-state formalism with a modified overlap matrix. It can be solved in the usual way and yields the one-particle states within the approximations of the LDF formalism and the variational freedom of the basis set.

In Fig. 4 the resulting band structures are compared with those eigenvalues that can be obtained by neglectation of the self-energy corrections, i.e., from the Schrödinger equation of the ground-state formalism. The deviations are rather small and exceed 0.3 eV only in the lowest valence band. These small deviations, which, however, become important for the quantitative comparison with ex-

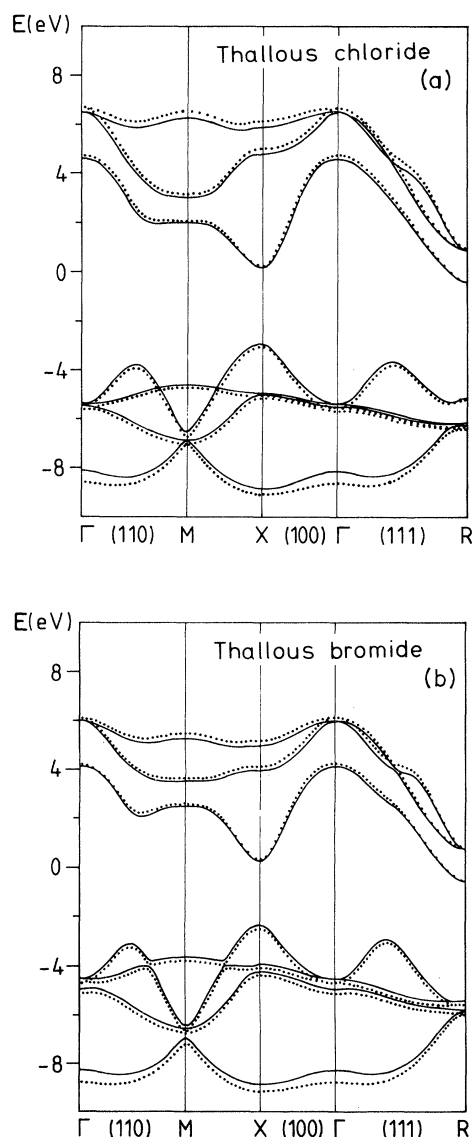


FIG. 4. Thallous halide band structures calculated with (solid lines) and without (dotted lines) self-energy corrections at the experimental equilibrium lattice constant.

perimental spectra, explain the success of band structures⁸⁻¹⁰ which were obtained from the ground-state equation only, a procedure which is strictly speaking incorrect as discussed in the Introduction.

A common deficiency of LDF band-structure calculations, even including self-energy corrections, is a considerable undervaluation of the band gaps^{10,26-28} compared with optical experiments. This drawback, which we shall also observe in the next section, has usually been attributed to self-interaction: The Coulomb and exchange-interaction terms of one orbital with itself do not cancel in the LDF formalism in contrast to the Hartree-Fock ansatz. For finite systems *ad hoc* corrections were justified and successfully implemented.²⁸⁻³⁰ The application of these corrections to infinite systems however is by no means straightforward. Besides states which are localized by impurities²⁶ or otherwise,³¹ the eigenstates of a crystal are Bloch functions for which those interaction terms vanish in the thermodynamic limit.^{17,32} Therefore we believe that self-interaction corrections cannot repair the mentioned deficiency.

III. BAND STRUCTURES

We now turn to the analysis of the band structures for thallose chloride and thallose bromide in Fig. 4, which have been calculated *ab initio* without any fitting parameter in the described way. Qualitatively they agree with band structures obtained earlier from Korringa-Kohn-Rostoker (KKR),³³ pseudopotential,³⁴ linear combination of atomic orbitals (LCAO),³⁵ and orthogonalized-plane-wave (OPW) (Ref. 36) calculations. Quantitatively the comparison with experimental data shows much better overall agreement than those calculations.

In agreement with those earlier calculations, our valence bands predominantly consist of thallium *s* and halogen *p* states, while the conduction bands are built from thallium *p* states. This partition could be expected from the ground-state investigation,² where only a small mixing of Tl *p* states into the ground-state charge density was observed, i.e., Tl *p* states remained largely unoccupied in the ground state. Among the valence bands, on the other hand, a considerable mixing between *s* and *p* orbitals localized on nearest-neighbor sites leads to a large dispersion, which is maximal at the *X* point as expected from symmetry arguments. Accordingly, the top of the valence bands occurs at the *X* point, and the states display predominant

s character with 30–40% halogen *p* contribution. Similarly pure *p* conduction bands should obtain minima at points *X*, *M*, and *R*. While the minimum at point *M* is prevented by relatively strong mixing of valence-band states, we do find distinct minima of the conduction bands at points *X* and *R*. As a consequence we obtain a direct gap at point *X* and an indirect gap between points *X* and *R* (see Fig. 4) in agreement with experimental observations.³⁷⁻³⁹ This usual feature of gaps at the edge of the Brillouin zone follows therefore directly from the electronic configuration of the ten-electron compounds with their surplus *s*-electron pair. In contrast the respective *s* states in alkali halides, for example, belong to the conduction bands so that symmetry arguments alone explain a direct gap at Γ .

The optical absorption at the direct gap of the thallose halides is hence dominated by an intracationic transition; the following two structures in the absorption spectra⁴⁰ can be attributed to transitions from the second and third valence band to the lowest conduction band at the *X* point, and these are therefore interionic transitions with a corresponding charge transfer from halogen to thallium ions. This unambiguous assignment follows from the spin-orbit coupling of the halogen states, which agrees not only with the splitting of the structures in the absorption spectra but also with the distance between the bands in the band structure.

In Table I we compare the energies of the discussed transitions with the experimental values. The agreement is very good for the spin-orbit-split doublet, the differences between chloride and bromide direct and indirect gaps are also correctly reproduced, but the calculated direct gaps are too small by 0.3 eV, and the indirect gaps are too small by another 0.4 eV.

We have been able to attribute more than half of this discrepancy to the discussed neglect of the dispersion of core-orthogonalization terms.¹⁷ The remaining error of 0.1 eV for the direct and 0.3 eV for the indirect gaps are surprisingly small compared to other LDF calculations. The reason for this unexpected accuracy is not clear at the moment. We have already disclaimed the usual pretext by means of self-interaction terms in the preceding section. The essential difference between our calculation and other applications of the LDF formalism is the extreme high atomic number of thallium, this may suggest that the undervalued band gaps are a consequence of an unknown systematic error which decreases with increasing number

TABLE I. Energetic distance of critical points of the thallose halide band structures in Fig. 4 compared to the respective energies of optical transitions [S. Kurita and K. Kobayashi, *Proceedings of the Tenth International Conference on the Physics of Semiconductors, Cambridge, 1970*, edited by S. Keller, J. Hensel, and F. Stern (United States Atomic Energy Commission, Oak Ridge, 1970), p. 171; R. Z. Bachrach and F. C. Brown, *Phys. Rev. B* **1**, 818 (1970); and Reference 38]. All values are given in eV.

	Thallose chloride		Thallose bromide	
	Theory	Experiment	Theory	Experiment
Direct gap	3.09	3.42	2.65	3.02
Indirect gap	2.50	3.22	1.81	2.67
Spin-orbit-split doublet	5.12	4.92	4.21	4.05
	5.18	5.02	4.52	4.47

of electrons.

For a discussion of the pressure dependence of the optical transitions we calculate the band structures for smaller than the equilibrium lattice constants. An example is shown in Fig. 5. The used lattice constant corresponds to a hydrostatic pressure of 29 kbar.⁴¹ As a consequence the dispersion of all bands increases, and the bands are shifted towards higher energies due to the increased kinetic energy. The last effect is stronger for *s* than for *p* states due to the comparatively smaller localization of the former. The increased Madelung energy shifts thallium states upwards and halogen states downwards. For the valence bands these effects largely cancel except for those states in the uppermost band which are dominated by thallium *s* contributions, because in this case, dispersion, kinetic energy, and Madelung shift all increase the energy. At the bottom of the conduction bands the increase is weakened by dispersion effects.

As a result the direct as well as the indirect gaps are reduced at the smaller lattice constant. This behavior, which we can thus directly derive from the electronic configuration characteristic for ten-electron systems with *s-p*-mixed valence bands and cationic *p* conduction bands, was already derived from nonself-consistent OPW calculations³⁶ and has also been observed experimentally.⁴²⁻⁴⁴ The measured pressure coefficients are presented in Table II. With respect to their largeness and their sign, they distinguish the thallos halides from other materials. The pressure coefficients of silver halides for example differ by a factor of -2.2 for the direct gaps and by a factor of 10.6 for the absorption edge.⁴³ The theoretical pressure coefficients contained in Table II are calculated from the band structures in Fig. 5 for thallos chloride and similarly for bromide, using the experimental pressure dependence of the lattice constant. As expected from Fig. 5 the pressure coefficients for the direct gap are large and negative and for the indirect gap, i.e., the absorption edge, they are even larger. The spin-orbit-split transition is nearly unchanged under pressure. These observations agree with experiments, but the calculated absolute values are even larger than the experimental data. Accordingly the deformation potentials are substantially overestimated. The effect of the wave-vector-independent core orthogonalization increases drastically with reduced lattice constant and thus contributes to these errors. But the main reason for these deviations is certainly the overvaluation of the repulsive potential in our calculation as discussed in I so that the reduced lattice constant corresponds to a higher hydrostatic pressure than the 29 kbar used in deriving the data in Table II. In fact, the deviations in Table II are cut

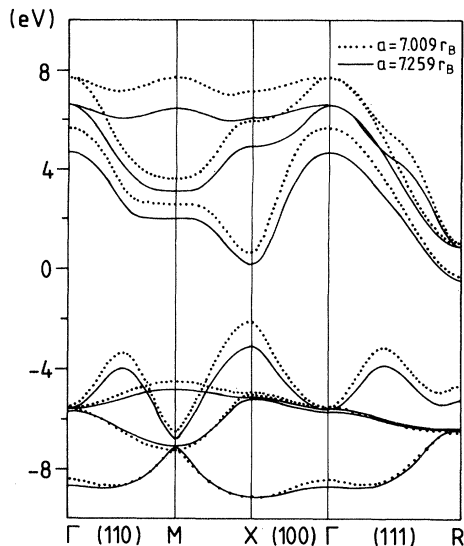


FIG. 5. Thallos chloride band structure calculated under neglect of self-energy corrections at the experimental equilibrium (solid lines) and at a reduced (dotted lines) lattice constant, simulating a hydrostatic pressure of 29 kbar.

in half if we calculate the pressure coefficients by means of the appropriate theoretical compressibility according to the total-energy curves in I.

IV. DENSITIES OF STATES

As a comparison of higher optical transitions with critical points of *ab initio* band-structure calculations is not justifiable,⁴⁵ we turn to the densities of states (DOS's) for further comparison with experiments. Extensive uv photoemission experiments have been published for thallos chloride⁴⁶; we shall compare the conclusion which those authors have drawn from the energy-distribution curves (EDC's) with the valence-band DOS curve which is shown in Fig. 6. The strong structures in the EDC's at 1.0 and 2.2 eV below the valence-band maximum (VBM) correspond to the high DOS at -0.9 and -2.3 eV. The high DOS at -3.3 eV appears as a weak shoulder at -3.4 eV in the EDC's for high incident-photon energy. Obviously these states are not fully recorded with the available photon energies. Near the VBM the DOS curves display a small shoulder; so do the EDC's at -0.3 eV for (8.9–9.2)-eV photons. Accordingly, at 8.6–8.9 eV above the VBM there should be conduction-band states close to

TABLE II. Pressure coefficients of the energies of the lowest optical transitions and volume deformation potentials of thallos halides.

Transition	Quantity	Thallos chloride			Thallos bromide		
		Theory	Experiments Ref. 44	Ref. 43	Theory	Experiments Ref. 44	Ref. 43
Indirect	dE/dp (10^{-6} eV/bar)	-28		-16	-36		-18
Direct	dE/dp (10^{-6} eV/bar)	-18	-8.6	-13.2	-20.8	-9.2	-13.7
Direct	$V dE/dV$ (eV)	+ 5.1	+ 2.4	+ 3.2	+ 5.4	+ 2.3	+ 3.0

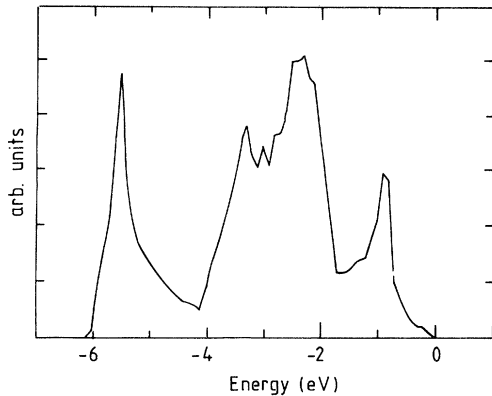


FIG. 6. DOS of the valence bands of thallos chloride corresponding to the band structure shown in Fig. 4. Energy scale is shifted so that the VBM is zero.

the X point of the Brillouin zone because valence-band states at -0.3 eV exist only near the X point. In fact, the highest conduction band at point X is separated from the VBM at 8.9 eV (see Fig. 4). For higher incident-photon energies the EDC's around -0.3 eV are particularly reduced, hence no conduction-band states should be expected near the X point 10 eV above the VBM. No states appear in Fig. 4 in this region; this observation indicates that at least at point X the higher conduction bands are separated from the computed bands by at least 0.8 eV. A more detailed analysis of the strong EDC peaks allows us to prove this statement for the whole Brillouin zone: The -1.0 -eV peak is strongest for $(8.6-9.2)$ -eV photons, and decreases from 9.6 eV until it nearly vanishes at 10.4 eV to reappear at 11.2 eV. The same behavior shifted by 1.2 eV is displayed by the -2.2 -eV peak. Correspondingly, the conduction-band DOS should be large around 8 eV above VBM, decrease from 8.6 to 9.4 eV and rise again at 10.2 eV. The DOS, which is presented in Fig. 7, does indeed show a maximum at 8.6 eV according to the uppermost band in Fig. 4 and the decrease towards 9.4 eV. Higher bands not considered in our calculation are of course responsible for the renewed rise in the EDC's.

All the above information, which was drawn from the EDC's by experimentalists,⁴⁶ is in good agreement with

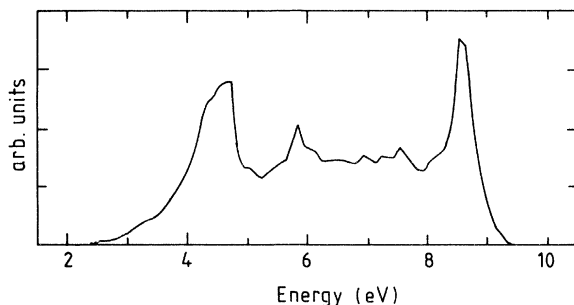


FIG. 7. DOS of the conduction bands of thallos chloride corresponding to the band structure shown in Fig. 4. (Bottom of the band is at 3 eV, the tailing is a numerical error due to the linear approximation of the Gilat-Raubenheimer procedure which was used in the integration over the Brillouin zone.)

the present investigation. Only one observation seems to contradict, namely, the valence-band width, which was given as 4 eV, although another weak structure at -4.5 eV was found in the EDC's for high photon energy and attributed to inelastically scattered electrons.⁴⁶ A comparison with the band structure in Fig. 4 suggests that this shoulder is caused by the lowest valence band. The matching maximum in the valence-band DOS is situated at -5.5 eV. Reexamination of the EDC's show that the structure increases with increasing incident-photon energy and shifts from -4.3 to -4.8 eV. This suggests that the highest incident-photon energy was still insufficient to determine the real position of this structure. A further increase and shift towards -5.5 eV can be expected.

This expectation is satisfied by x-ray and uv photoemission spectra at much higher energy (21.2 eV).⁴⁷ In Fig. 8 these experiments are reproduced and compared with the valence-band DOS which was broadened by convolution with a Gaussian to match the resolution of the experiments. All EDC structures are in good agreement with the theoretical results, in particular the discussed weak shoulder at -3.4 is now distinct and the lowest valence band shows up at -5.6 eV in the x-ray spectrum.

For a further corroboration of the conduction-band DOS, we analyze the results of core-level spectroscopy which were obtained for TlCl by the use of synchrotron radiation.⁴⁸ If we neglect the matrix elements, the absorption from the energetically sharp core level into the conduction bands should directly reflect the DOS of these bands.

The soft-x-ray (approximately 200 eV) absorption spectra start with an antiresonance reflecting the Fano effect occurring at the formation of the core exciton pertinent to the $2p$ level of chlorine against a continuous background which is here given by the absorption from $5p$, $5s$, and $4f$

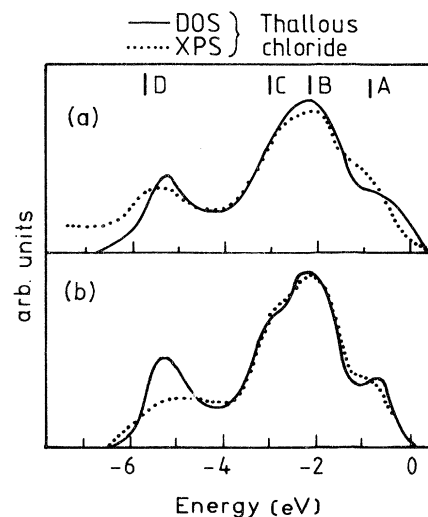


FIG. 8. Solid lines represent DOS's of the valence bands of thallos chloride (cf. Fig. 6), broadened by convolution with Gaussians of a halfwidth of (a) 0.9 eV and (b) 0.7 eV. Dotted lines represent photoemission spectra (Ref. 47) of TlCl ; (a) XPS ($\text{Al } K\alpha$), (b) UPS (21.2 eV without the background of inelastically scattered electrons).

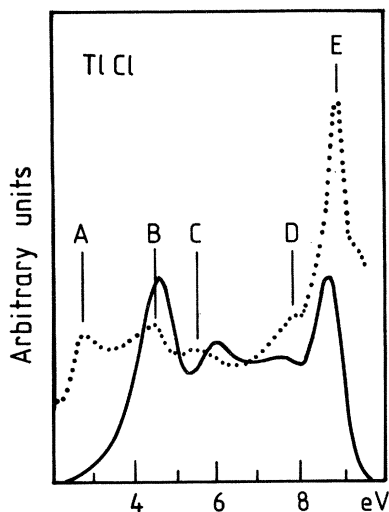


FIG. 9. DOS of the conduction bands of thallos chloride (cf. Fig. 7), broadened by convolution with a Gaussian of a half-width of 0.7 eV (solid line) in order to match the resolution of the soft-x-ray absorption spectra (Ref. 48) (dotted line).

states of thallium. Thus the first peak in these spectra corresponds to the conduction-band bottom, 1.7 eV above which we observe a strong structure, succeeded by weaker structures at 2.5 and 5 eV and a very large peak at 6 eV, which is followed by a distinct drop.⁴⁸ In the DOS (see Fig. 9) these observations match the strong peaks at 1.8 and 5.5 eV and weaker structures at 3.0 and 4.7 eV above the conduction-band minimum. We expect the core level of chlorine 2*p* to suffer a spin-orbit splitting of 1.8 eV. The commensurate doublets are reflected in the absorption spectra although some of the spin-orbit partners of the discussed absorption structures coincide with other peaks; the second exciton, for example, is not distinguishable from the 1.7-eV peak. For thallos bromide comparable photoemission experiments are complicated by surface charges⁴⁹ and by the satellites of core structures which are superimposed in the valence-band region.²³ A comparison of the available spectra^{23,49,50} with thallos chloride spectra does not show qualitative differences. The EDC's again display a weak shoulder at -0.4 eV and a shoulder at around -1.2 eV, followed by a strong maximum at -2.2 eV with a shoulder at -3.5 eV.⁵⁰ The experiments also show with regard to the conduction bands that the re-

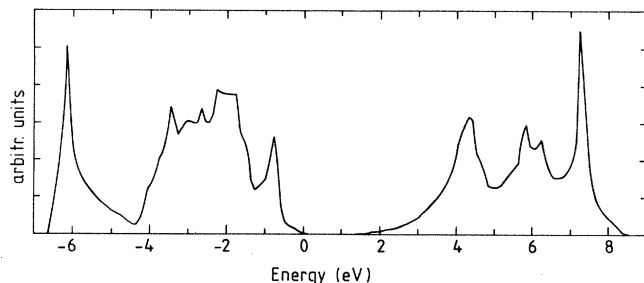


FIG. 10. DOS of thallos bromide corresponding to the band structure shown in Fig. 5. Energy scale is shifted so that the VBM is zero.

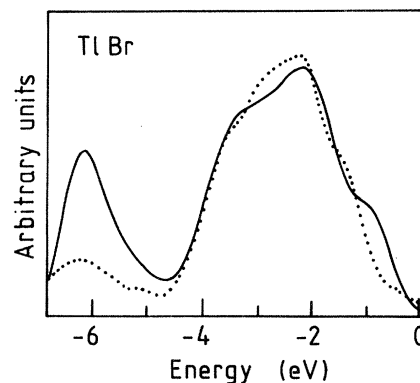


FIG. 11. DOS of the valence bands of thallos bromide (cf. Fig. 10), broadened by convolution with a Gaussian of a half-width of 0.7 eV (solid lines) in order to match the resolution of the x-ray photoemission spectra (Ref. 50) (dotted lines).

gion between 6.5 and 7.3 eV above the VBM stands out for its high DOS.⁴⁹ The theoretical results for thallos bromide are presented in Figs. 10 and 11. In the valence-band region the very weak shoulder at -0.3 eV, the peak at -0.9 eV, and the strong peak at around -2 eV with a shoulder up to -3.5 eV, all agree with the expectations from the experiment under discussion, and the maximum of the conduction-band DOS is also at 7.3 eV. In contrast to earlier measurements⁴⁹ the recent x-ray photoemission experiments⁵⁰ show an additional peak at -6.0 eV, which corresponds to the lowest valence band in Fig. 4 and is reflected by the strong peak at the bottom of the DOS at -6.0 eV in Figs. 10 and 11.

V. CONCLUSION

Together with the previous paper, the present investigation constitutes an *ab initio* self-consistent description of the electronic structure of simple cubic thallos halides. Without fitting any parameter we derived a consistent representation of the many-electron ground state and the one-particle states. Ground-state properties as well as many optical data have been calculated and shown to be in good agreement with experiments thus confirming the validity of our approach and the accuracy of our results. The numerical errors have been reduced below 0.1 eV for the one-particle energies. The deviations of our band structures and densities of states from experimental data are generally of the same size or, where they are larger, could be shown to relate to the usage of the frozen-core approximation. Therefore the methodological accuracy, in particular, the local-density approximation for the self-energy turned out to be the same as the achieved numerical accuracy. We conclude that the effect of nonlocal contributions to the self-energy is below 0.1 eV, while our calculations have shown that the consideration of the self-energy corrections in the local approximation is more important for the achieved overall agreement with experiments (a neglect of these corrections would increase most of the deviations by 0.1–0.2 eV). We believe that this accuracy, which is considerably higher than in previous investigations, is necessary for a realistic description of the electronic states with respect to further applications.

- ¹J. Treusch, Phys. Rev. Lett. **34**, 1343 (1975).
- ²M. Schreiber and W. Schäfer, preceding paper, Phys. Rev. B **28**, 2238 (1983).
- ³P. Hohenberg and W. Kohn, Phys. Rev. **136**, B864 (1964).
- ⁴W. Kohn and L. J. Sham, Phys. Rev. **140**, A1133 (1965).
- ⁵L. J. Sham and W. Kohn, Phys. Rev. **145**, 561 (1966).
- ⁶L. Hedin, S. Lundquist, in *Solid State Physics*, edited by F. Seitz, D. Turnbull, and H. Ehrenreich (Academic, New York, 1969), Vol. 23, p. 1.
- ⁷T. Koopmans, Physica (Utrecht) **1**, 104 (1933).
- ⁸C. C. Pei, Phys. Rev. B **18**, 2583 (1978).
- ⁹J. Kübler, J. Phys. F **8**, 2301 (1978).
- ¹⁰A. Zunger and M. L. Cohen, Phys. Rev. B **20**, 1189 (1979).
- ¹¹W. Schäfer and M. Schreiber, Solid State Commun. **38**, 1241 (1981).
- ¹²G. Wannier, Phys. Rev. **52**, 191 (1937).
- ¹³W. Andreoni, Phys. Rev. B **14**, 4247 (1976).
- ¹⁴W. Kohn, Phys. Rev. B **7**, 4388 (1972).
- ¹⁵M. Schreiber and W. Schäfer, Phys. Rev. B **21**, 3571 (1980).
- ¹⁶L. Hedin and B. I. Lundquist, J. Phys. C **4**, 2064 (1971).
- ¹⁷M. Schreiber, Doktor thesis, Universität Dortmund, 1980 (unpublished).
- ¹⁸J. Des Cloizeaux, Phys. Rev. **129**, 554 (1963); **135**, A685 (1964); **135**, A698 (1964).
- ¹⁹C. Tejedor and J. A. Vergés, Phys. Rev. B **19**, 2283 (1979).
- ²⁰P. O. Löwdin, J. Chem. Phys. **18**, 365 (1950).
- ²¹The calculation of the band structures in this investigation was performed for the experimental lattice constant. The equilibrium lattice constants determined from the minimization of the total energy in I are too large because of the overestimation of the repulsive potential due to the frozen-core approximation. A variation of these core functions, however, would change the total energy much more than the one-particle states of valence and conduction bands, as was discussed with respect to the basis-set convergence in I. Therefore the assumption is justified that an optimization of the core functions, which should yield the minimum of the total energy at the experimental equilibrium lattice constant, would only slightly influence the band structure as compared to the frozen-core calculation at this lattice constant.
- ²²R. T. Poole, J. D. Riley, D. R. Williams, J. G. Jenkin, R. C. G. Leckey, and J. Liesegang, J. Phys. **8**, 3636 (1975).
- ²³D. R. Williams, R. T. Poole, J. G. Jenkin, J. Liesegang, and R. C. G. Leckey, J. Electron Spectrosc. Relat. Phenom. **9**, 11 (1976).
- ²⁴D. A. Liberman, D. T. Cromer, and J. T. Waber, Comput. Phys. Commun. **2**, 107 (1971).
- ²⁵For details about the actual computation of the matrix elements we refer to the description in Refs. 15 and 17.
- ²⁶A. Zunger and A. J. Freeman, Phys. Rev. B **16**, 2901 (1977).
- ²⁷A. Zunger and A. J. Freeman, Phys. Rev. B **17**, 4850 (1978).
- ²⁸A. Zunger and M. L. Cohen, Phys. Rev. B **18**, 5449 (1978).
- ²⁹O. Gunnarson, B. I. Lundquist, and J. W. Wilkins, Phys. Rev. B **10**, 1319 (1974).
- ³⁰K. Schwarz, Chem. Phys. Lett. **57**, 605 (1978).
- ³¹S. Doniach, in *Computational Methods in Band Theory*, edited by P. M. Marcus, J. F. Janak, and A. R. Williams (Plenum, New York, 1971), p. 500.
- ³²R. A. Heaton, J. G. Harrison, and C. C. Lin, Solid State Commun. **41**, 827 (1982).
- ³³H. Overhof and J. Treusch, Solid State Commun. **9**, 53 (1971).
- ³⁴M. Inoue and M. Okazaki, J. Phys. Soc. Jpn. **31**, 1313 (1971).
- ³⁵J. Overton and J. P. Hernandez, Phys. Rev. B **7**, 778 (1973).
- ³⁶J. P. van Dyke and G. A. Samara, Phys. Rev. B **11**, 4935 (1975).
- ³⁷E. Mohler, G. Schlögl, and J. Treusch, Phys. Rev. Lett. **27**, 424 (1971).
- ³⁸I. Nakahara, K. Kobayashi, and A. Fujii, J. Phys. Soc. Jpn. **37**, 1312, **37**, 1319 (1974).
- ³⁹J. Nakahara and K. Kobayashi, J. Phys. Soc. Jpn. **40**, 180 (1976).
- ⁴⁰H. Zinngrebe, Z. Phys. **154**, 495 (1959).
- ⁴¹*Landolt-Börnstein, Numerical Data and Functional Relationships in Science and Technology*, edited by K. H. Hellwege (Springer, Berlin, 1973).
- ⁴²J. Zahner and H. G. Drickamer, J. Phys. Chem. Solids **11**, 92 (1959).
- ⁴³A. D. Brothers and D. W. Lynch, Phys. Rev. **180**, 911 (1969).
- ⁴⁴A. J. Grant, W. Y. Liang, and A. D. Yoffe, Philos. Mag. **22**, 1129 (1970).
- ⁴⁵W. Hanke, Adv. Phys. **27**, 287 (1978).
- ⁴⁶S. F. Lin and W. E. Spicer, Phys. Rev. B **14**, 4559 (1976).
- ⁴⁷J. Kanbe, H. Onuki, and R. Onaka, J. Phys. Soc. Jpn. **43**, 1280 (1977).
- ⁴⁸S. Sato, M. Watanabe, Y. Iguchi, S. Nakai, Y. Nakamura, and T. Sagawa, J. Phys. Soc. Jpn. **33**, 1638 (1972).
- ⁴⁹L. Laude (private communications).
- ⁵⁰L. Porte, J. Chem. Phys. **73**, 1104 (1980).